Experimental Verification of Improved Two Port Hybrid High Gain Buck Boost Converter based Dynamic Voltage Restorer (PV-DVR) System for Social Welfare

D.C. Kumaresan and Dr.P. Selvan

Abstract--- *Energy saving has become an active research area and it is essential to take out system faults to ensure the efficient functioning of the overall system. The power quality issues concerned with voltage sag and they frequently cause serious power interruptions in varied industrial applications. These industrial problems have its impact in terms of economic and social welfare. This work presents a novel PhotoVoltaic fed Dynamic Voltage Restorer (PV-DVR) model to alleviate deep voltage sags and outages on a low voltage residential distribution system. The application of low step up and high step up DC–DC converters used in the existing DVR system results in high conversion loss. Moreover, two control loops are required to control the two separate converters which results in higher control complexity. Thus, in this proposed work, Two Port Hybrid High Gain Buck Boost Converter (TPHGC) is integrated in the existing PV-DVR system. Two converters used in the existing system are replaced with single battery charging bidirectional converter. Simulation results are presented to validate the advantage of the proposed system.*

Keywords--- *DVR, Reactive Power, Compensation, Controller, Maximum Power Point Tracking (MPPT) Algorithm.*

I. INTRODUCTION

Owing to perturbations or fluctuations in recent years, the power quality that gets transmitted or distributed has tend to become less. Faults in the power system can lead to voltage sag or swell in the complete system or only a major portion of it. Additionally, harmonics, voltage transients, flickers count one among the voltage quality issues Jing et al. (2008). Voltage sag can happen at any point of time that ranges from 0.1 to 0.9 p.u and lasting for half a cycle to one minute Francis and Thomas (2014). Voltage sag can again be either balanced or unbalanced chiefly depending on the kind of fault. The important sources of voltage sag are any kind of fault observed in the power system or when the huge motor loads are started. Importantly, voltage sags are treated to pose considerable menace to the power quality. In a similar manner, the voltage swells can happen at any point of time ranging from 1.1 to 1.8 p.u and lasting for half a cycle to one minute. But the frequency of voltage swells are less in comparison with that of voltage sags that are largely generated due to the abrupt switching off of huge loads or the capacitor banks energization Hingorani and Gyugyi (2000). Because of these faults, under the conditions of full load, it may lead to critical or higher voltage drops in the system. Also because of these perturbations, system has to go through a

---

D.C. Kumaresan, Department of EEE, Karpagam University, Coimbatore. E-mail:dckumaresan@gmail.com
Dr.P. Selvan, Department of Electrical and Electronics Engineering, Erode Sengunthar Engineering College, Thudupathi, Erode.

shutdown or failure inclusive of huge voltage and current imbalances present in the system. Several methods has to be followed or employed by the customer for mitigating these voltage sags / swells in order to have a better quality of power supply for the equipment so that it functions effectively. But, the effects of the voltage sag or swell to the equipment might become costly to the customer. There are several strategies that are available for compensating the voltage sag and swell, where the custom power device installation is the suitable technique for mitigating the voltage sag and swell. This idea of installation of the custom power device is being suggested by Hingorani in 2000. Installing the custom power device refers to the usage of power electronic controllers in the power system to manage the different power quality issues. The important aim to tackle with different power quality problems is guaranteeing the users with a better quality and reliable supply. There are multiple custom power devices that are available for rendering solution to the various power quality challenges, though DVR is treated to be the most appropriate solution for mitigating the voltage sag and swells intruding the power system Bollen (2003); Moreno-Munoz et al. (2010).

The idea observed in Ashari et al. (2007) is the DVR usage is addressing the problems of the voltage sags and improvement in the outage while the PV system is absent. In Sasitharan et al. (2007) is shown the series injection transformer's architectural design along with its rating. There are different researches which have been carried out focusing over the design and control system of the DVR Jowder (2009). The on-line type of DVR as it is studied in Han et al. (2007) has been rendered in view of compensation for the system's voltage sag. In the case of electrical distribution system, the DVR that has no PV system, is propped up additionally by the energy storage tool that acts as the super capacitor and assists in the power quality improvement as introduced in Omar and Rahim (2012). The PV operated DVR has the part of working out the compensation for the system's voltage sag as observed in Al-Mathnani et al. (2007). In the above seen DVR models, there exists no customer advantages monetary wise. Hence, a PV-DVR model is proposed that gets over the disadvantages of the models above mentioned. This technical work has been considered to be the inspiration of this research work. The chief goal of this work is the design of a modified converter section shown in Ramasamy and Thangavel (2013).

The conventional PV-DVR block diagram of Ramasamy and Thangavel (2013) is shown in Figure 1. In this existing PV_DVR system, two types of converters namely low step up and high step up have been used Mohan et al (2007); Hsieh et al. (2013). To control the low step up DC–DC converter, the P&O MPPT algorithm is used Reisi et al. (2013); Femia et al. (2003); Lalili et al. (2011). Similarly, in order to control the high step up DC-DC converter, outer voltage control based closed loop system is used. These two conversions results in high conversion loss as two converters are used in the existing system. The battery presented in this existing system charges through low step up converter where as the discharging operation takes place through high step up converter. Thus, two converters are used in this existing system. Moreover, a charging controller has also been used to state of charge (SOC) of the battery as shown in Figure 1. Three controlling techniques are used. The battery charger controller with two bypasses switches R_1 and R_2 has been used in the existing system. Considering a scenario, wherein the battery gets fully charged, the excess voltage from the PV array may not be utilized by the battery which results in wastage of power. Thus, in the existing system, the efficiency gets reduced with increased control complexity. On the other hand, the cost and system size also gets increased.

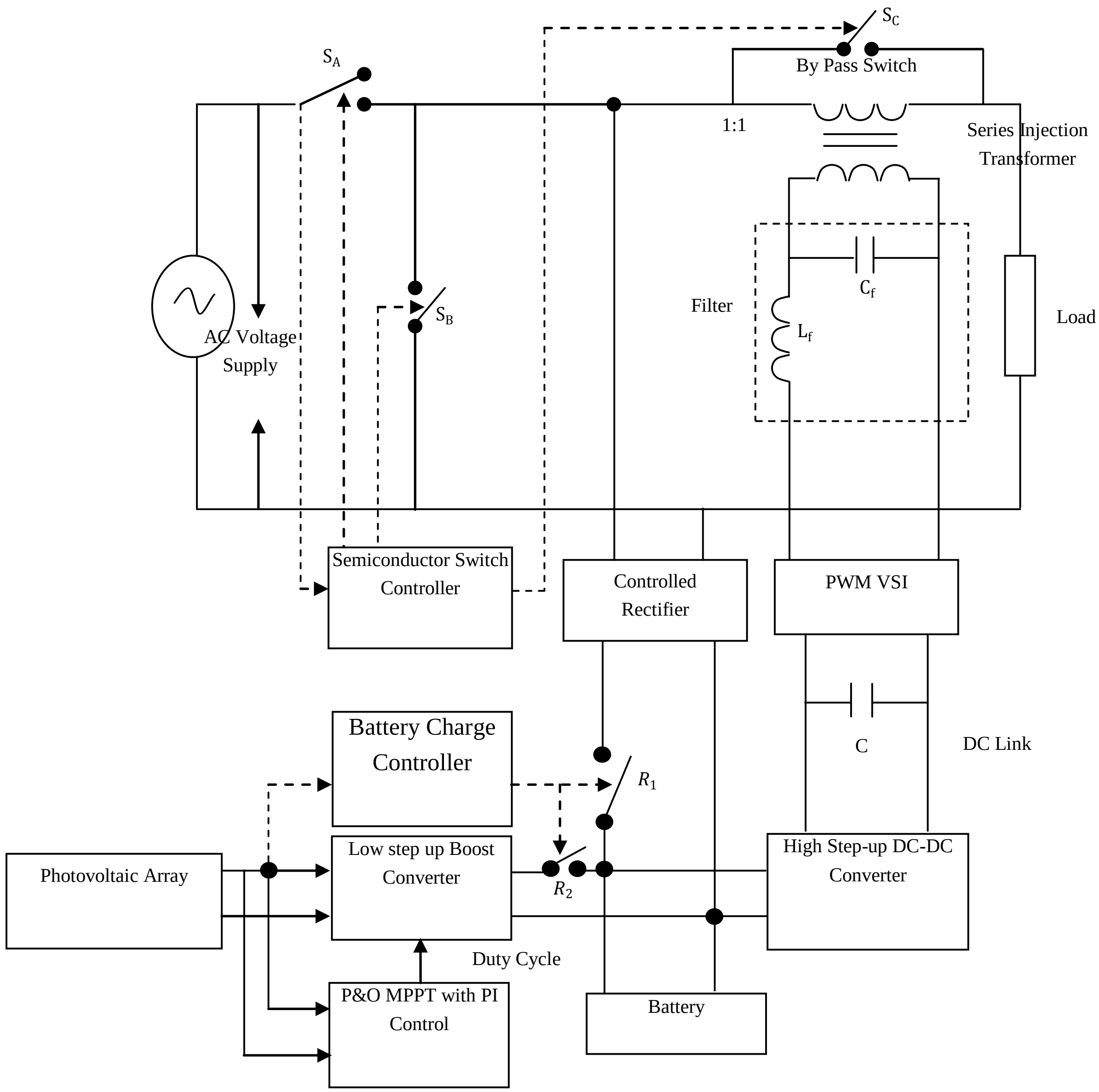

Figure 1: Block Diagram of Conventional PV-DVR

The battery charge control logic is shown in Table 1.

Table 1: Battery Charge Control

PV voltage in volts	Control Signal		Battery charging unit
	R_1	R_2	
>6	0	1	PV array
<6	1	1	Rectifier and PV array

The main purpose of this research work is to overcome the drawbacks of the existing system, two port hybrid high gain buck boost converter (TPHGC) is integrated in the existing PV-DVR system. In this proposed PV-DVR system, PV array and battery represent the two port section. Two converters used in the existing system are replaced with single battery charging bidirectional converter as shown in Figure 2.

The proposed PV-DVR system operates in three modes of operations as described below.

1. PV Power = Output Power (Ideal)
2. PV Power > Output Power (Battery Charging)
3. PV Power < Output Power (Battery Discharging)

II. SYSTEM DESCRIPTION

Figure 2 shows the proposed PV-DVR architectural design with the novel TPHGC. The proposed PV_DVR system comprises of the battery, a PV array, PWM inverter, and series injection transformer, TPHGC and semiconductor switches marked as S_A, S_B & S_C. Normally S_A and S_C are closed and S_B open when grid voltage is a state of normal. On the other hand, when S_A and S_C are open and S_B is closed, then system acts in UPS mode. Similarly, sag compensation mode occurs when S_A is closed, S_B&S_C are open.

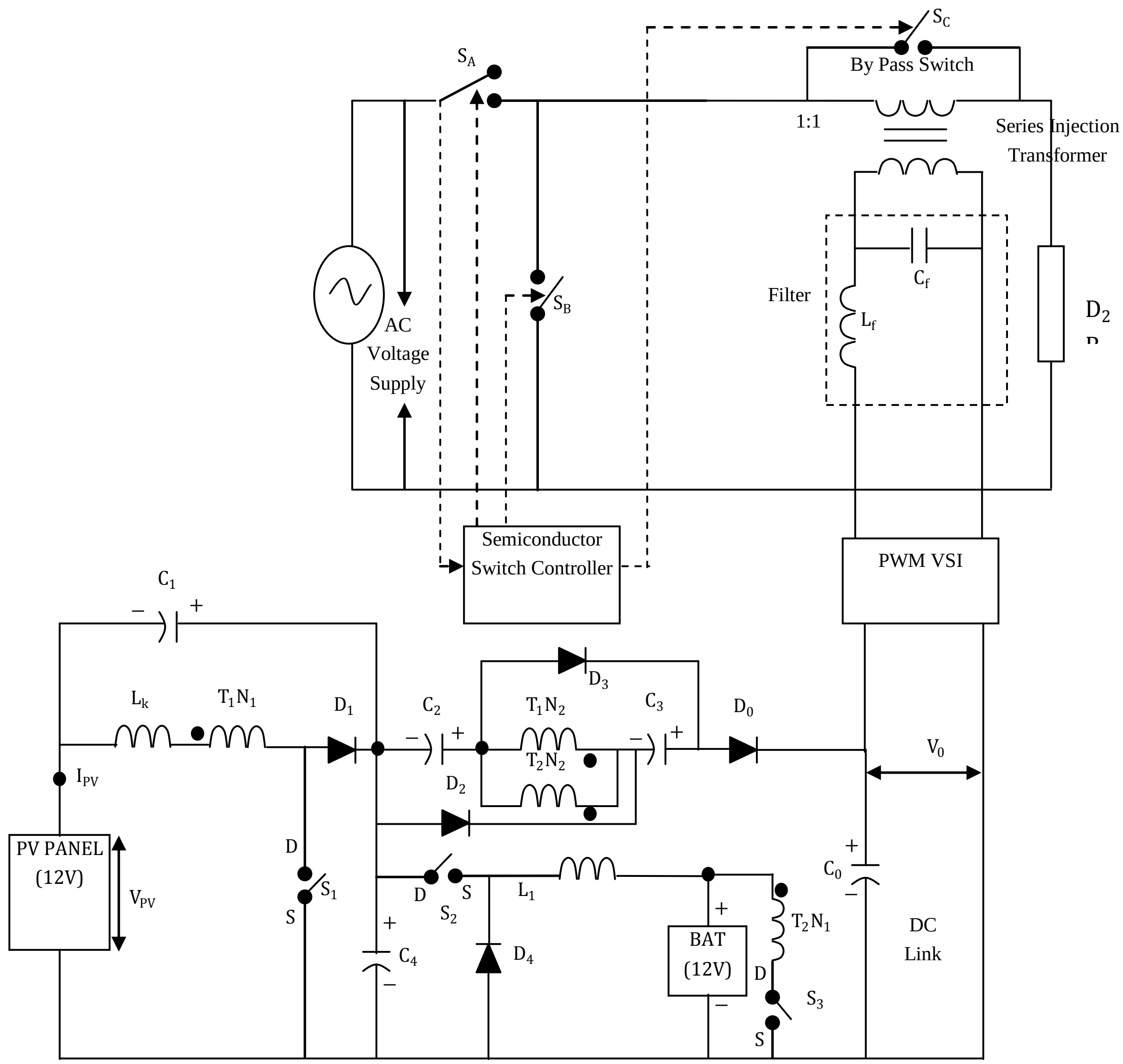

Figure 2: Proposed TPHGC Based PV-DVR System

Table 2 shows the semiconductor's control signals as switches S_A, S_B&S_C. The functioning of the proposed PV-DVR in three modes is discussed in detail:

1. The idle or maintenance mode: The PV-DVR during this mode is completely disconnected in the semiconductor switch $S_C$course. This is done in the secondary by passing the injecting transformer wherein maintenance is required by the DVR.
2. The compensation mode also known as DVR mode: Proposed PV-DVR in the compensation mode is used to bring in a state of voltage regulation in the load side. In this process the load basically compensates voltage sags are configured sequentially in the series injection transformer.
3. Uninterruptible Power Supply (UPS) mode: During the UPS mode, PV-DVR series injection transformer is basically configured again as parallel so that it supplies the load with an uninterruptible power supply both during the day as well at night.

Table 2: Control Signal forS_A, S_B and S_C

Supply Voltage in %	Control Signal			Mode of Operation
	S_A	S_B	S_C	
100	1	0	1	idle
<100	1	0	0	DVR
0	0	1	0	UPS

Mode of Operation

i. PV power=Load power

Five Mode of operation is shown in Figure 3. This mode of operation clearly describes the condition when the load power is met (satisfied) by the PV power.

Mode 0

In this mode ($S_1 = \mathrm{ON}$), initially the current from PV flows through the transformer T_1N_1 and the switch S_1 to get neutralized. Thus, the current flow through the transformer T_1N_1 , creates a flux which in turn generates the current flow in the secondary winding of the transformer T_1N_2. At this point of time, two circulating paths are created which charges capacitor C_2 and C_3.

The current flowing path for charging the capacitor C_2 is initiated from the secondary winding of the transformer T_1N_2 and charges the capacitor C_2 then flows through the diode D_2 which completes the circulating path.Similarly, the current flowing path for charging the capacitor C_3 is initiated from the secondary winding of the transformer T_1N_2 and flows through the diode D_3 and then charges the capacitor C_3 which completes the circulating path.

Mode 1

The initial current flowing path of Mode 1 is same as discussed in Mode 0. At this time, extra current in the inductance flows through the capacitors C_1 and C_2 and energies the secondary winding of the transformer T_1N_2. Then the current flows through capacitor C_3. Thus, the capacitor C_1, C_2 and C_3 are in series and stores the voltage in capacitor C_0 which results in high gain mode operation.

At this point, a circulating path is created which charges the capacitor C_4 through the capacitor C_1 and gets neutralized at PV.

ii. PV power=Load Power

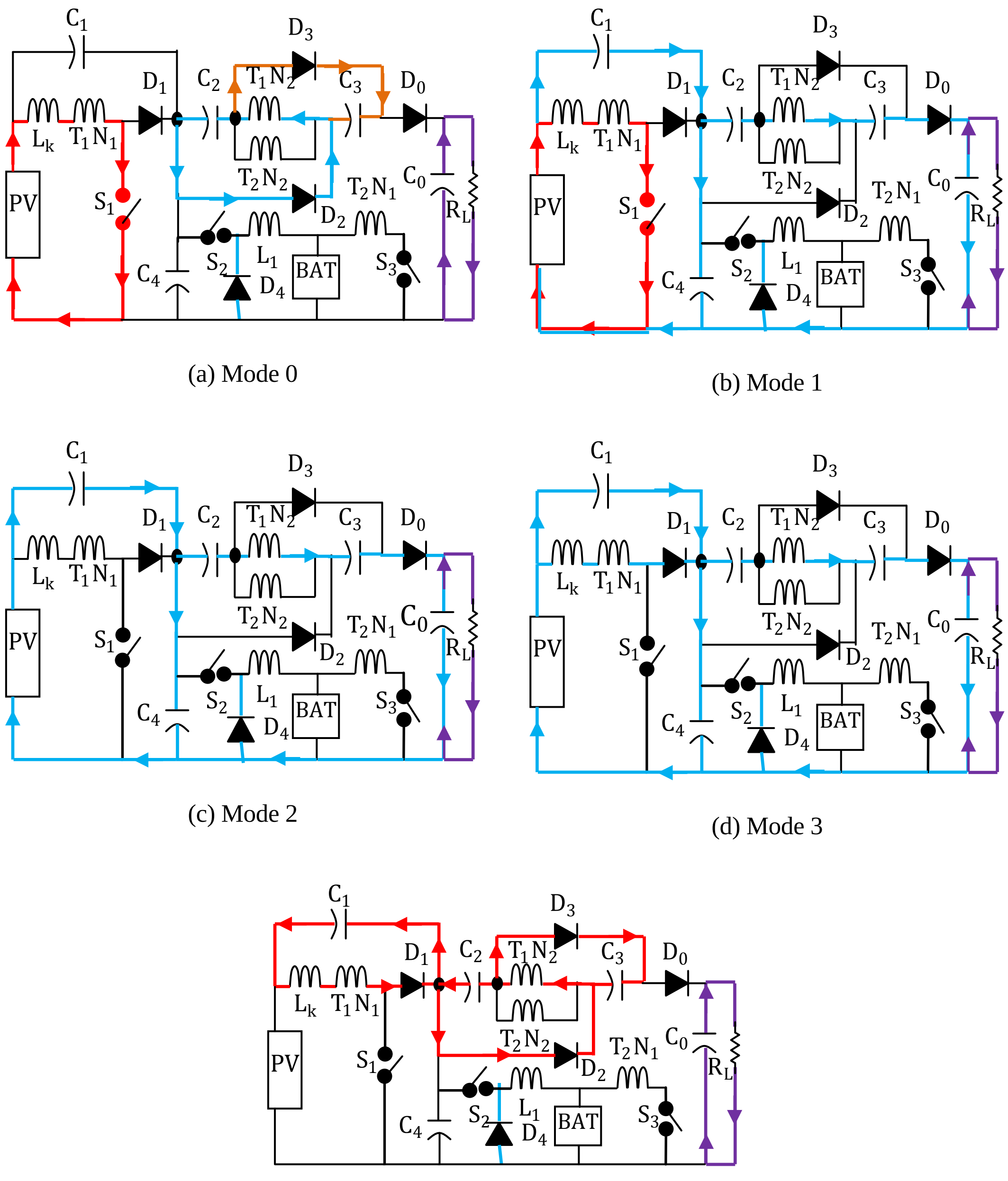

(a) Mode 0

(b) Mode 1

(c) Mode 2

(d) Mode 3

(e) Mode 4

Figure 3: Mode of Operation PV power=Load Power

Mode 2

In this mode S_1 is in OFF condition. This mode is almost similar to the mode 1, which is based on the linear discharge of T_1N_2 as shown in Figure 3 (c).

Mode 3

This mode is also called as leakage inductor discharge mode. This is same as the mode 2 but leakage inductance of the transformer gets discharged through diode D_1 and stores the voltage across the capacitor C_0 and gets neutralized at PV as shown in Figure 3(d).

Mode 4

In this mode, capacitor C_1 is in full discharged condition. Now, the voltage stored in the capacitor C_1 gets discharged and energies the transformer T_1N_1 and flows through the diode D_1 and gets neutralized. At this point, current through the transformer T_1N_1 creates a flux which in turn generates the current flow in the secondary winding of the transformer T_1N_2 which in turn produces two circulating paths (C_2&C_3 capacitor charging) as mentioned in mode 0 as shown in Figure 3(e).

iii. PV power>O/P power

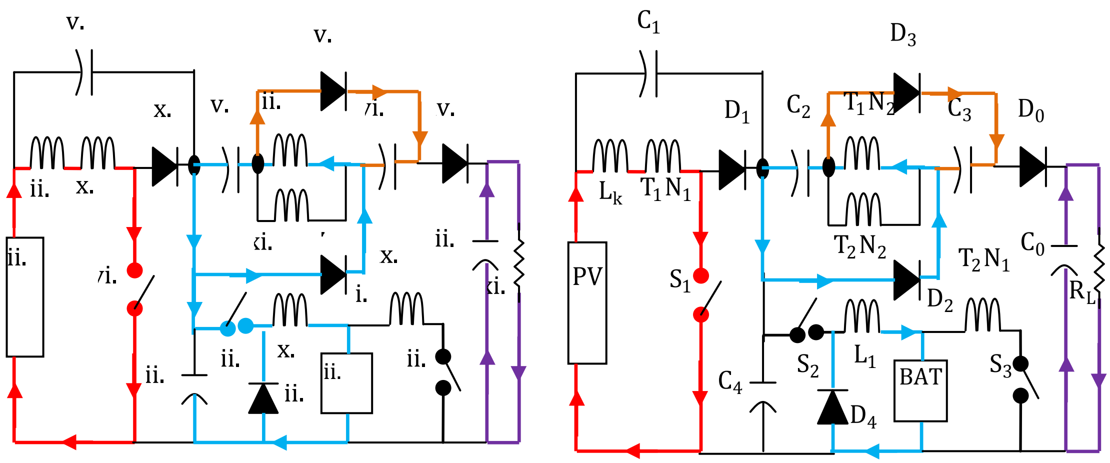

(a) Mode 5 (b) Mode 6

Figure 4: Mode of Operation PV power>Load Power

In this 'PV power>O/P power' condition, the generated PV power is greater than the load power and now, this excess PV power is efficiently stored in the battery through the buck mode of operation. All modes of operations (Mode 0 to Mode4), occurred in PV power=load power condition, is same for this operation. Moreover, controlling the switch S_2in the proposed converter is the main aspect which makes the change over from the previous "PV power=load power" condition. At the time when excess power is sensed in the system, switch S_2 is in ON condition. Based on the previous mode of operation, capacitor C_4 is in fully charged condition and when the switch is closed it results in increase of current, and an opposing voltage across its terminals is generated by the inductor due to the varying current. This voltage drop cancel outs the voltage of the source and thus minimizes the net voltage across the battery. In the mode (5), the current from C_4 flows through the inductance L_1 and charges the battery which then gets neutralized at capacitor C_4as shown in Figure 4 (a) mode 5. In mode 6, when switch S_2 is in OFF condition, the inductance L_1 completely discharges through the diode D4 to charge the battery as shown in Figure 4(b) mode 6.

iv. PV power<O/P power

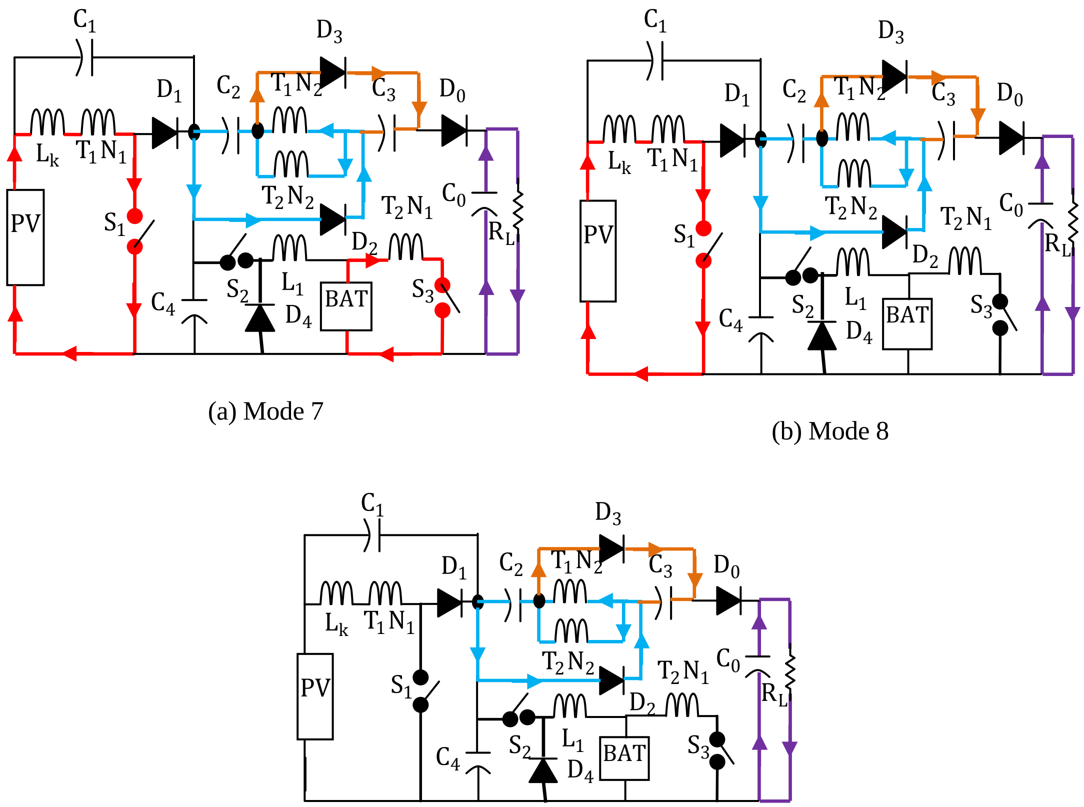

(a) Mode 7

(b) Mode 8

(c) Mode 9

Figure 5: Mode of Operation PV power<Load Power

In this 'PV power<O/P power' condition, the generated PV power is lesser than the load power and now, in order to meet the load demand, the stored power from the battery is discharged to meet the required load demand based on the controlling technique as shown in Figure 3 (b).At this discharging condition, boost operation is carried out to meet the load demand.

All modes of operations (Mode 0 to Mode 4), occurred in PV power=load power condition, is same for this operation. This mode of operation initiates with switch S_3 in ON condition. Thus, the current from the battery flows the primary winding of the transformer T_2N_1 and then flows through the drain source of switch S_3 and gets neutralized.

Due to the current flow in the primary winding of the transformer T_2, flux is created at the secondary winding of the transformer T_2. Based on the previous modes, when the switch $S_1$is in ON condition, the flux gets generated at the transformer T_1. Now, the flux generated at T_1 and T_2, simultaneously charges the capacitors C_3 and C_2respectively which acts in series connection and support the load demand as shown in Figure 5 (a) (mode 7).

In mode (8), switch S_3 is in OFF condition, remaining flux in transformer T_2 gets discharged and simultaneous, switch S_1 becomes OFF state which in turn makes the remaining flux in transformer T_1 to get discharged fully to support the load demand. The end of this cycle leads to the beginning of the next cycle (PV power = Load power).

Two Port Hybrid High Gain Buck Boost Converter (TPHGC) Control

In this MPPT conversion, P&O algorithm has been used for attaining the maximum power from the PV panel. The working of this P&O algorithm is mainly based on voltage and power. P&O algorithm works on the principle that, if there is increase in power, then the perturbation is maintained in the same direction and on the other hand, if there is decrease in the power, then the perturbation should be maintained in the opposite direction. This process is iterated until the maximum power point is reached.

A triangular carrier signal is generated with a switching frequency of 10 KHz as depicted in Figure 6 (a). Duty cycle from the P&O algorithm and the carrier signal is compared to generate the PWM pulse. Based on this control operation, the PV voltage is boosted up through the MPPT to meet up the load voltage demand.

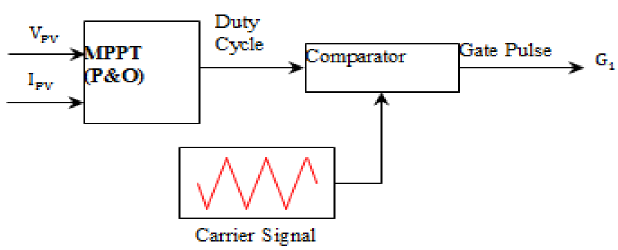

(a) Maximum Power Point Tracking (MPPT)Control

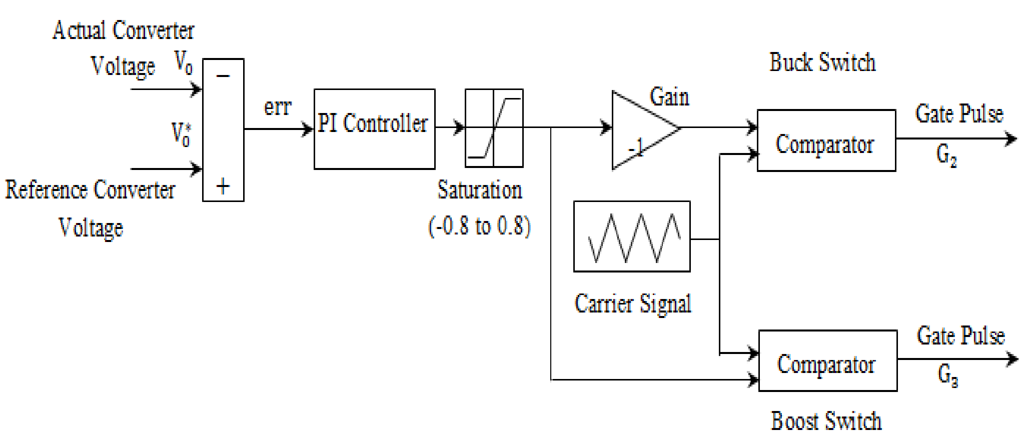

(b) Outer Voltage Control Loop

Figure 6: Closed loop Control of TPHGC

Figure 6(b) shows the outer voltage control with battery charging and discharging control loop. The battery charging and discharging is based on the load voltage. Thus, when the load voltage is high, the battery discharging operation is carried out by controlling the switch S_3. On the other hand, when the load voltage is lower, the battery charging operation is carried out by controlling the switch S_2 which is clearly depicted in Figure 6(b).

In this work, the actual and reference TPHGC voltage is compared and output error is given to the PI controller for controlling operation. The voltage error from the proposed converter is taken as feedback to control the dc link voltage of the inverter. Thus, with this closed loop control system, the input voltage of inverter in the DVR is maintained constant.

A proportional Integral (PI) is control loop feedback mechanism used in industrial control system. In industrial process a PI controller attempts to correct that error between a measured process variable and desired set point by calculating and then outputting corrective action that can adjust the process accordingly.

The PI controller calculation involves two separate modes the proportional mode, integral mode. The proportional mode determine the reaction to the current error, integral mode determines the reaction based recent error. The weighted sum of the two modes output as corrective action to the control element. PI controller is widely used in industry due to its ease in design and simple structure. PI controller algorithm can be implemented as

$$\mathrm{output}\ (t) = K_P\ \mathrm{err}\ (t) + K_I \int_0^t \mathrm{err}\ (\tau) d\tau \quad (1)$$

Where

$$\mathrm{err}\ (t) = \text{set voltage} - \text{actual voltage}$$

The output error from the controller is limited through a saturation limit unit which is assigned between (-0.8 to +0.8). In this work, a positive carrier signal is generated with 0 to 1 amplitude. Now, when the error output is negative, then error is multiplied with the negative Gain factor. Now, the negative error and the negative gain are multiplied to generate a positive error and are compared with the positive carrier to generate a G_2 gate pulse which acts in buck switching (charging) mode.

On the other hand, when there is positive error from the controller, then error is compared with the positive carrier signal and there is no need to multiply the gain factor in this scenario. Now, the positive error is compared directly with the positive carrier to generate a G_3 gate pulse which acts in boost switching (discharging) mode. Thus it is to be concluded that the gate pulses G_2 and G_3 are always in inverse active mode wherein when switch S_2 is ON, switch S_3 would be in OFF state and vice verse.

A. Photovoltaic Array Modeling

A system which comprises of solar cells that produce electricity through the process of conversion of sunlight forms a PV array or a photovoltaic array. Through the MPPT algorithm new efficient solar cells have been developed which has led to the increase of the solar panel use as an alternate renewable source of energy. The PV array along with the MPPT methodology through the low step up DC converter in the proposed DVR has become the DVR inverter's DC voltage source. This lies between DC link's battery bank and the PV.

Designing of the PV array is carried out by deploying the photovoltaic cells' basic equations along with solar irradiation level and effects of changes in temperature Altas and Sharaf (2007). The PV cell's output voltage is basically one of the photo current's functionalities and which is primarily determined by amount of load current which in turn depends on the level of solar radiation El-Tayyan (2011). PV cell output voltage is calculated as per the following:

$$V_c = \frac{AkT_c}{e} ln\left(\frac{I_{ph} + I_0 - I_c}{I_0}\right) - R_s I_c \tag{2}$$

$$V_{PV} = V_c \times N_s \tag{3}$$

$$I_c = \frac{I_{PV}}{N_p} \tag{4}$$

Here e refers to the electron's charge $(1.602 \times 10^{-19} c)$, V_c the output voltage of PV cell in volts, I_0 refers to the reverse saturation current of diode $(48.10 \times 10^{-19}$ A), k is Boltzmann constant (1.38×10^{-23} J/0K), I_c is the cell output current in A, N_s is the number of series cell (9), R_s is the cell internal resistance $(0.210\,\Omega)$, A refers to the curve fitting factor (1.23), I_c is the operating temperature of the reference cell (25 0C), V_{pv} is the output voltage of PV array, I_{ph} is the photo current in A (8.07 A), I_{pv} is the output current of the PV array and N_p is the number of parallel cells (6).

B. DVR PI Controller

The control scheme used to maintain a constant voltage magnitude at the load point, under system disturbance, is shown in Figure 7. In the proposed controller, a discrete single phase PLL is used to track the phase angle of the source voltage to perform the parks transformation on the measured single phase voltage. The measured p.u. value of supply voltage is converted into |Vs|, and the error is obtained from the difference of |Vs| and reference voltage (Vref). The PI controller designed by the Ziegler–Nicholstuning method processes the error and generates required angle d to drive the error to zero. The modulating angle d is applied to the reference voltage generator to generate the Vref for the Sinusoidal Pulse Width Modulation (SPWM). The reference voltage calculation is obtained by the following equation

$$V_{ref} = |V| * Sin(\omega t + \delta) I_c \tag{5}$$

The generated Vref is utilized to produce switching pulses for Voltage Source Inverter(VSI). The basic idea of Sine Pulse Width Modulation (SPWM) is to compare a sinusoidal control signal (Vref) of normal frequency 50 Hz with a triangular carrier waveform (Vcarrier) with 20 kHz signal to produce the PWM pulses. When the control signal is greater than the carrier signal, the switches are turned on, and their counter switches are turned off. The output voltage of the inverter mitigates the voltage sag.

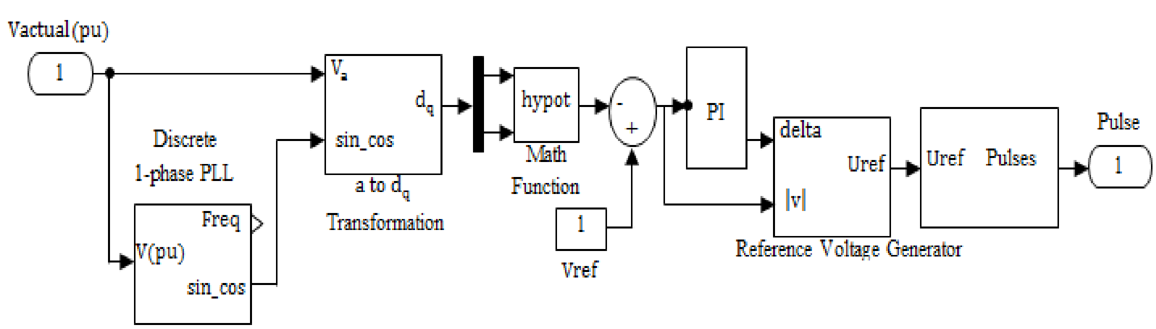

Figure 7: Control Structure of DVR

C. In-phase Voltage Compensation Method

In general, there are essentially three techniques deployed that include in-phase, the minimal energy injection method and presage so that DVR injection voltage maybe calculated. The paper basically discusses the in-phase compensation method deployed so that DVR. The injection voltage can be measured, as it is simple in terms of the implementation and also quick responsive nature when computing the compensating voltage. The DVR capabilities to be able to compensate for the voltage drop through the process of injecting voltage through deploying the source voltage in the in-phase series injection transformer El-Shennawy et al. (2010). As in Figure 8 injected voltage in the secondary that runs through the series injection transformer is actually in the in-phase along with the supply voltage.

In a state of normalcy, in an angle of zero phase, load and supply voltage (V_{presag}) are equal. At the time of voltage sags, the supply voltage decreases to a value less than or greater than the existing nominal value. As a result DVR counteracts to voltage sags and then injects required compensating in-phase voltage V_{inj} in- along with the supply voltage so that the voltage may be restored to normalcy as at its nominal value. Injected DVR (V_{inj}) voltage may be expressed as follows:

$$|V_{\mathrm{inj}}| = |V_{\mathrm{presag}}| - |V_{\mathrm{sag}}| \tag{6}$$

$$V_{\mathrm{DVR}} = V_{\mathrm{inj}} \tag{7}$$

$$|V_{\mathrm{DVR}}| = |V_{\mathrm{presag}}| - |V_{\mathrm{sag}}| \tag{8}$$

Calculation of injected voltage angle may be done as per the following equation:

$$< V_{\mathrm{inj}} = \theta_{\mathrm{inj}} = \theta_s \tag{9}$$

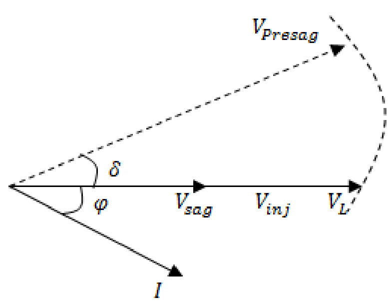

Figure 8: In-Phase Compensation to Presagvoltage

D. Voltage Sag Detection using d-q Transformation

V_a isthe supply voltage gets transformed as positive sequence's d-q values in the proposed sag detection method. V_{smax} is acquired by deploying single-phase d-q transformation theory Lira et al. (2006). The component referred to as d which is part of the d-q transformation is equal to the DC value equivalent to the AC source voltage peak. Assuming that line voltage being the ideal sinusoidal waveform, the d-q theory assumes the generation of real and imaginary signal as follows Kumaresan DC and Selvan (2016):

$$V_{real}(t) = V_{smax}\ \sin(\omega t) \quad (10)$$

$$V_{image}(t) = -V_{smax}\ \cos(\omega t) \quad (11)$$

Here

$V_{real}(t)$, $V_{image}(t)$ is the real and imaginary part of $V_s(t)$, V_{smax} is the AC source voltage peak value.

The d-q transformation can be expressed as

$$\begin{bmatrix} V_d \\ V_q \end{bmatrix} = \begin{bmatrix} \sin(\omega t) & -cos(\omega t) \\ cos(\omega t) & sin(\omega t) \end{bmatrix} \begin{bmatrix} V_{real} \\ V_{image} \end{bmatrix} \quad (12)$$

From the transformation as shown above we obtain the following values $V_d = V_{smax}$ and $V_q = 0$. There is an inherent delay that is an outcome under natural circumstances; however the delay is minimal in comparison to system response under voltage swells, sags or outages. Monitoring of V_d, returns the voltage drop and rise and the manipulation of Vq will return the initial phase jump information.

III. SIMULATION RESULTS

This Simulation of the proposed work has been carried out in MATLAB. Results from the simulation have further been evaluated. During the initial phase evaluation of the park transformation results has been performed.

V_{smax} is the distorted voltage where the voltage suddenly drops which would result in SAG voltage.

Figure 9 shows the voltage sag compensation of the proposed system in both DVR and UPS mode. In DVR mode, the proposed system acts as DVR wherein the voltage sag is compensated in the presence of input AC supply.

Figure 9 shows the resultant waveforms of the proposed system as a DVR. Figure 9 (a) shows the SAG voltage waveform of the proposed system. It is observed from the figure that, at time 0.3 second, voltage sag of 50 V_{rms} is observed in the system. So, it means that, 250 V_{rms} has to be injected in the system to compensate the voltage sag. This injected voltage waveform is clearly shown in Figure 9 (b). Figure 9 (c) shows the load voltage waveform at the voltage sag condition. It is observed that, at 0.2 second, there is sudden drop in load voltage due to the voltage sag. But, suddenly at 0.23 second, the voltage sag is compensated due to the injected voltage. Figure 9 (d) shows the State Of Charge (SOC) battery at the voltage sag condition. It is clearly shown that, at the voltage sag condition, the battery is in discharging condition from (0.2 to 0.4 seconds). The battery operates in charging condition except in sag condition.

When there is no input AC supply, the proposed system acts as UPS wherein the DVR will inject the voltage in this condition in order to make the load voltage constant. Figure 9 (e) shows the deep SAG voltage (0 V) waveform of the proposed system. It is observed from the figure that, at time 0.2 second, deep voltage sag of 0 Volt is observed in the system. So, it means that, 300 V_{rms} have to be injected in the system to compensate the deep voltage sag. This injected voltage waveform is clearly shown in Figure 9 (f). Figure 9 (g) shows the load voltage waveform at the deep voltage sag condition. It is observed that, at 0.2 second, load voltage is zero due to the deep voltage sag condition. But, suddenly at 0.23 second, the voltage sag is compensated due to the injected voltage. Figure 9 (h) shows the state of charge (SOC %) of the battery at the voltage sag condition. It is clearly shown that, at the deep voltage sag condition, the battery is in discharging condition from (0.2 to 0.4 seconds). The battery operates in charging condition except in sag condition. Figure 9 (i) shows the SOC of battery comparison of the two different conditions. It is observed that, in the UPS mode, battery discharging is higher when compared with the DVR mode to maintain the load voltage constant.

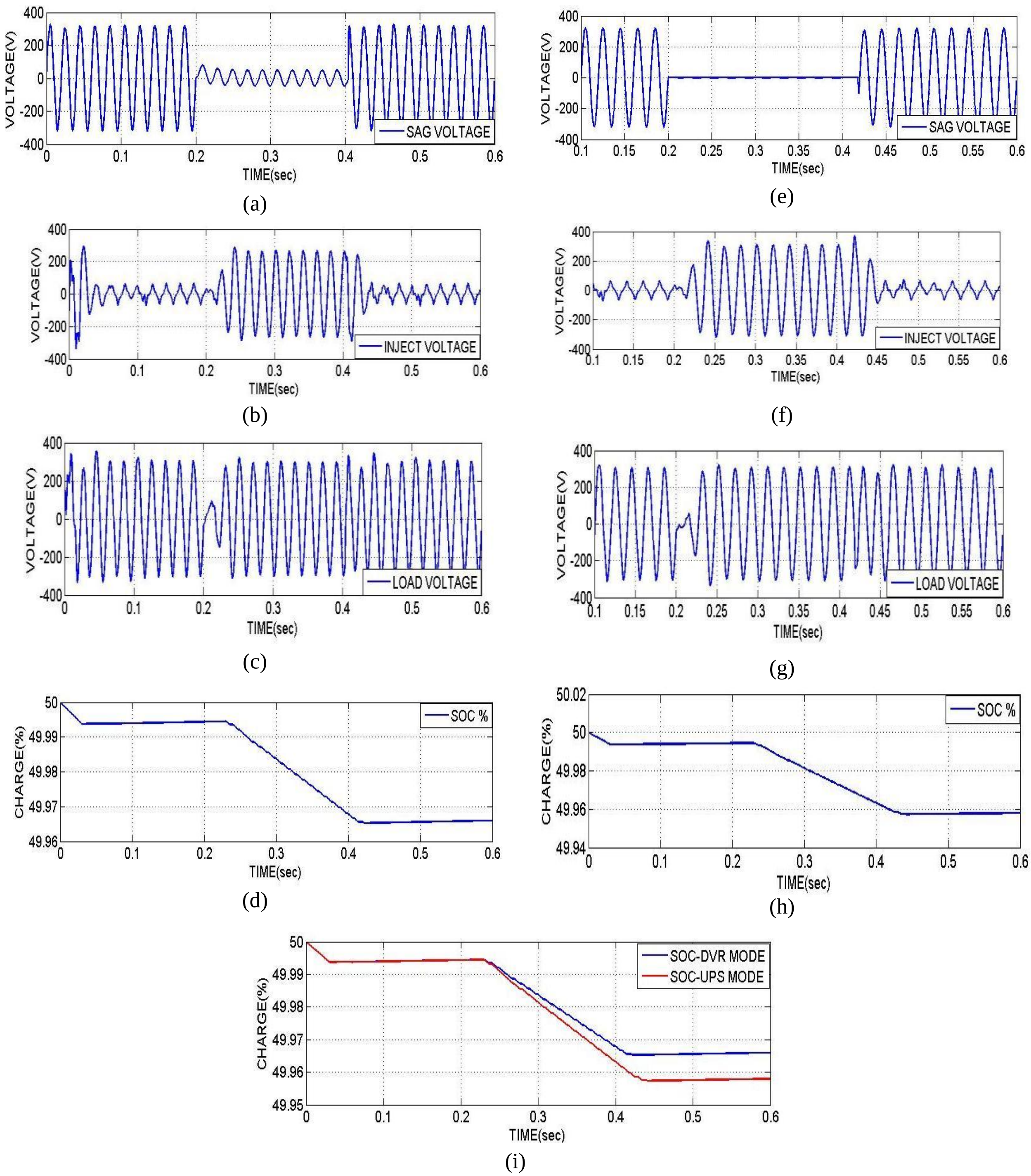

Figure 9: Evaluation Results of Proposed System in (1) DVR Mode and (2) UPS Mode

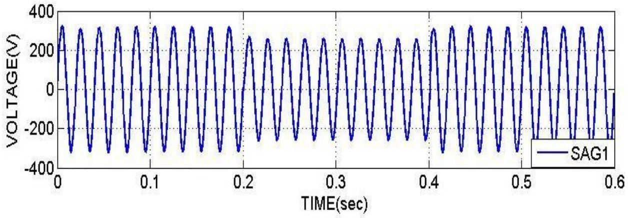

(a)

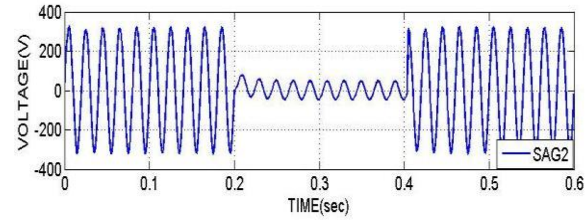

(c)

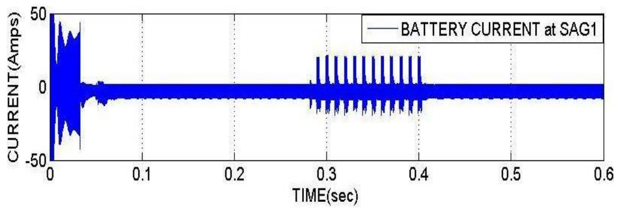

(b)

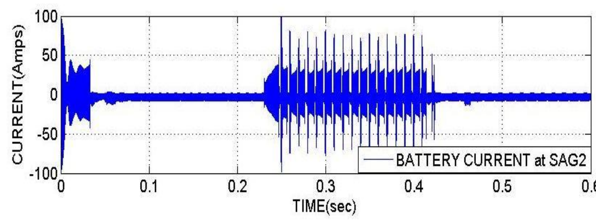

(d)

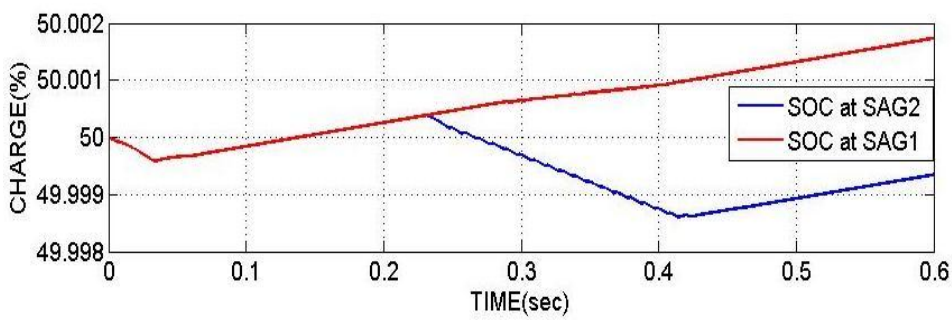

(e)

Figure 10: Evaluation Results of Battery Current and SOC% at Different SAG Conditions

Figure 10 shows the evaluation results of the battery current and SOC at two different SAG conditions. Figure 10 (a) shows the SAG1 condition wave form of the proposed system wherein 25% sag is created. Thus,75V_{rms} have to be injected in the system to compensate the voltage sag. Figure 10 (b) shows battery current waveform at the SAG condition. It is observed that, charging and discharging condition takes place at particular interval. Discharging takes place to compensate the sag condition. Since, 25% sag is created, only minimal injected is required and thus, the remaining voltage is effectively stored in the battery in the charging condition as depicted in Figure 10 (b).

Figure 10 (c) shows the SAG2 condition waveform of the proposed system wherein 75% sag is created. Thus, 200V_{rms} have to be injected in the system to compensate the voltage sag. Figure 10 (d) shows battery current waveform at the SAG2 condition. It is observed that, charging and discharging condition takes place at particular interval. Maximum discharging takes place to compensate the sag condition. Since, 75% sag is created, maximum injection is required and thus, the only minimal voltage is stored in the battery in the charging condition as depicted in Figure 10 (d).

Figure 10 (e) shows the State of Charge (SOC) of the battery at the voltage sag1 and Sag2 conditions. It is clearly shown that, at the voltage sag1 condition, the battery is in charging condition from (0.2 to 0.31 seconds). This is due to the minimal injection required, but at 0.32 second, there is a slight discharging condition which is depicted in the figure. But after 0.4 second, there is again a linear increase in the system which is due to the charging condition of the battery. Similarly, for the SAG2 condition, since maximum injection is required due to the sag, discharging takes place from the battery till 0.4 seconds, then after 0.4 seconds, charging takes place which is depicted by the increased linear curve.

A. Experimental Setup

The performance of the proposed TPHGC based PV-DVR model is experimentally validated on a developed hardware prototype as shown in Figure 11. A developed hardware prototype mainly comprises of 16 bit digital signal controller (dsPIC30F4011), MOSFET driver circuit for front end Two Port Hybrid High Gain Buck Boost Converter (TPHGC) and VSI switches, Hardware arrangement of TPHGC and VSI for power factor correction (PFC) and speed control operation respectively.

Figure 11: Hardware Result

B. MOSFET Driver Circuit for TPHGC based PV-DVR

The switching signal for a MOSFET is usually generated by a logic circuit or a microcontroller, which provides an output signal that typically is limited to a few mill amperes of current. Consequently, a MOSFET which is directly driven by such a signal would switch very slowly, with correspondingly high power loss. During switching, the gate capacitor of the MOSFET may draw current so quickly that it causes a current overdraw in the logic circuit or microcontroller, causing overheating which leads to permanent damage or even complete destruction of the chip. To prevent this from happening, a MOSFET driver is provided between the microcontroller output signal and the power MOSFET. The MOSFET driver unit mainly comprises of transistor BC547, optocoupler 6N135 and MOSFET driver IC ICL7667 as shown in Figure 12.

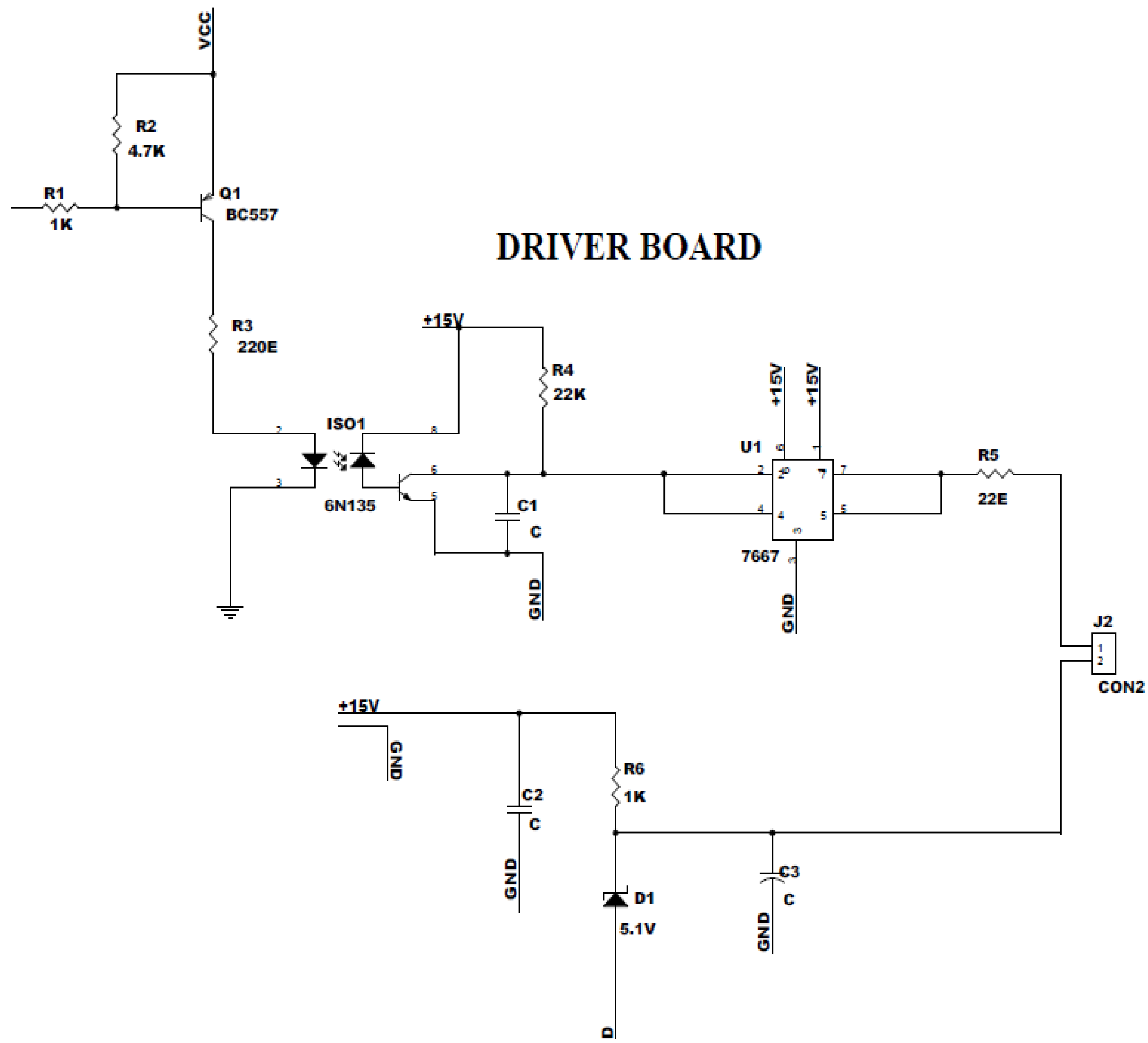

Figure 12: MOSFET Driver Circuit

In MOSFET driver unit BC547 is commonly used to amplify current. It is an NPN bi-polar junction transistor. A transistor, stands for transfer of resistance, a small current at its base controls a larger current at collector & emitter terminals. BC547 is mainly used for amplification and switching purposes. It has a maximum current gain of 800. The transistor terminals require a fixed dc voltage to operate in the desired region of its characteristic curves. This is known as the biasing. It is used in common emitter configuration for amplifiers.

Similarly the optocoupler TOSHIBA 6N135 consists of an AlGaAs LED optically coupled to a high speed photo detector transistor. A separate connection for the bias of the photodiode improves the speed by several orders of magnitude over conventional phototransistor optocouplers by reducing the base-collector capacitance of the input transistor. An internal noise shield provides superior common mode rejection of 10kV/μs. An improved package allows superior insulation permitting a 480V working voltage compared to industry standard of 220V. The pin configuration and package sketch of 6N135 optocoupler as shown in Figure 13.

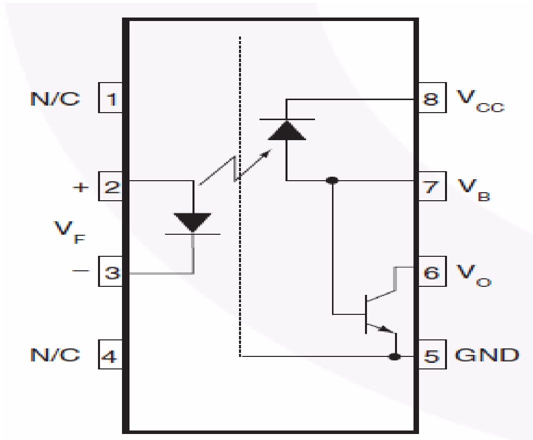

Pin diagram of 6N135

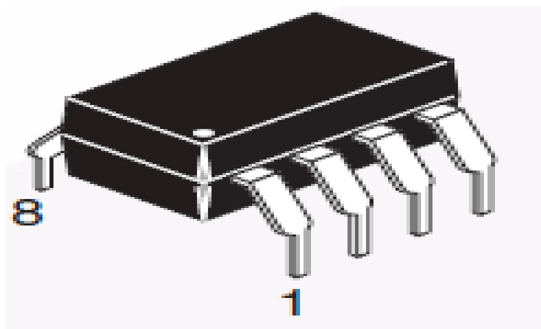

Package sketch of 6N135

Figure 13: Optocoupler (6N135) Schematic Diagram

In MOSFET driver unit, the role of driver IC ICL7667 is used to maximizing the switching speed. The ICL7667 is a dual monolithic high-speed driver designed to convert TTL level signals into high current outputs at voltages up to 15V. Its high speed and current output enable it to drive large capacitive loads with high slew rates and low propagation delays. With an output voltage swing only millivolts less than the supply voltage and a maximum supply voltage of 15V, the ICL7667 is well suited for driving power MOSFETs in high frequency switched-mode power converters. The ICL7667's high current outputs minimize power losses in the power MOSFETs by rapidly charging and discharging the gate capacitance. The ICL7667's inputs are TTL compatible and can be directly driven by common pulse-width modulation control ICs. The pin configuration of ICL7667 is shown in Figure 14.

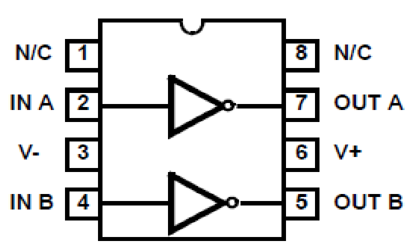

Pin Diagram of ICL7667

Package Sketch of ICL7667

Figure 14: Driver IC (ICL7667) Schematic Diagram

IV. CONCLUSION

This paper presents a novel approach and application that deploys a PV solar system to address voltage swells, sags and outage improvement through DVR for both residential and small scale industrial purposes. A novel TPHGC with single battery charging bidirectional conversion operation has been proposed in this work to overcome the limitation of the existing DVR system. The PV-DVR has been designed such that it reduces consumption of energy consumption from the main utility grid by basically detaching the utility grid from the load using several semiconductor switches. This is carried out once the PV array produces real power that is an equivalent amount or in excess in terms of the required load demand. Additionally, it has a twofold benefit as it reduces panel tariff and also aid in avoiding UPS and stabilizer use for personal individual residential use, small scale industrial purposes and at other educational institutions. The results from the experiments conducted and the simulation process show PV-DVR capability in terms of mitigating variations in voltage.

REFERENCES

[1] W. Jing, X. Aiqin and S. Yueyue, “A survey on control strategies of dynamic voltage restorer”, 13th International Conference on Harmonics and Quality of Power, Pp.1-5, 2008.

[2] D. Francis and T. Thomas, “Mitigation of voltage sag and swell using dynamic voltage restorer”, 2014 Annual International Conference on Emerging Research Areas: Magnetics, Machines and Drives (AICERA/iCMMD), Pp.1-6, 2014.

[3] G. Nagain and L.G. Hingorani, “Understanding FACTS: Concept and technology of flexible AC transmission systems”, 2000.

[4] M.H.J. Bollen, “What is power quality?”, Electric Power Systems Research, Vol.66, No.1, Pp.5-14, 2003.

[5] A. Moreno-Munoz, J.J.G. De-la-Rosa, M.A. Lopez-Rodriguez, J.M. Flores-Aries, F.J. Bellido-Outerino and M. Ruiz-de-Adana, “Improvement of power quality using distributed generation”, Int J Electr Power Energy System, Vol.32, No.10, Pp.1069–76, 2010.

[6] M. Ashari, T. Hiyama, M. Pujiantara, H. Suryoatmojo and M.H. Purnomo, “A Novel Dynamic Voltage Restorer with Outage Handling Capability Using Fuzzy Logic Controler”, Second International Conference on Innovative Computing, Information and Control, Pp.51-51, 2007.

[7] S. Sasitharan, M.K. Mishra, B. Kalyan Kumar and V. Jayashankar, “Rating and design issues of DVR injection transformer”, International Journal of Power Electronics, Vol.2, No.2, Pp.143-163, 2010.

[8] F.A. Jowder, “Modeling and simulation of different system topologies for dynamic voltage restorer using simulink”, International Conference on Electric Power and Energy Conversion Systems, Pp.1-6, 2009.

[9] J.H. Han, J.G. Shon, I.D. Seo and H.J. Jeon, “Development of on-line type dynamic voltage compensation system using super capacitor”, 7th Internatonal Conference on Power Electronics, Pp.455-460, 2007.

[10] R.O.S.L.I. Omar and N.A. Rahim, “Voltage unbalanced compensation using dynamic voltage restorer based on super capacitor”, International Journal of Electrical Power & Energy Systems, vol.43, No.1, Pp.573-581, 2012.

[11] A.O. Al-Mathnani, A. Mohamed and M.A.M. Ali, “Photovoltaic based dynamic voltage restorer for voltage

sag mitigation", In Research and Development, Pp.1-6, 2007.

[12] M. Ramasamy and S. Thangavel, "Experimental verification of PV based dynamic voltage restorer (PV-DVR) with significant energy conservation", International Journal of Electrical Power & Energy Systems, Vol.49, Pp.296-307, 2013.

[13] N. Mohan and T.M. Undeland, "Power electronics: converters, applications, and design", John Wiley & Sons, 2007.

[14] Y.P. Hsieh, J.F. Chen, T.J. Liang and L.S. Yang, "Novel high step-up DC–DC converter for distributed generation system", IEEE Transactions on Industrial Electronics, Vol.60, No.4, Pp.1473-1482, 2013.

[15] A.R. Reisi, M.H. Moradi and S. Jamasb, "Classification and comparison of maximum power point tracking techniques for photovoltaic system: A review", Renewable and Sustainable Energy Reviews, Vol.19, Pp.433-443, 2013.

[16] N. Femia, G. Petrone, G. Spagnuolo and M. Vitelli, "Optimization of perturb and observe maximum power point tracking method", IEEE transactions on power electronics, Vol.20, No.4, Pp.963-973, 2005.

[17] D. Lalili, A. Mellit, N. Lourci, B. Medjahed and E.M. Berkouk, "Input output feedback linearization control and variable step size MPPT algorithm of a grid-connected photovoltaic inverter", Renewable energy, Vol.36, No.12, Pp.3282-3291, 2011.

[18] I.H. Altas and A.M. Sharaf, "A photovoltaic array simulation model for Matlab-Simulink GUI environment", International Conference on Clean Electrical Power, Pp.341-345, 2007.

[19] A.A. El-Tayyan, "PV system behavior based on datasheet", Journal of Electron Devices, Vol.9, No.20011, Pp.335-341, 2011.

[20] T.I. El-Shennawy, A.M. Moussa, M.A. El-Gammal and A.Y. Abou-Ghazala, "A dynamic voltage restorer for voltage sag mitigation in a refinery with induction motors loads", Vol.3, No.1, Pp.144–51, 2010.

[21] J. Lira, C. Nunez, M. Flota and R. Alvarez, "A Control Strategy to Improve Voltage Sag Ride-Through in Single-Phase Multilevel Active Rectifier", 3rd International Conference on Electrical and Electronics Engineering, Pp.1-4, 2006.

[22] D.C. Kumaresan and P. Selvan, "Novel Hybrid High Gain Buck Boost Converter based Energy Saving PI Controller with Photovoltaic Fed Dynamic Voltage Restorer (PV-DVR) System", Asian Journal of Research in Social Sciences and Humanities, Vol.6, No.11, Pp.610-629, 2016.